THE EUROPEAN
PHYSICAL JOURNAL D

Regular Article

Multiple scattering of slow muons in an electron gas

Claudio Darío Archubi[1,a] and Nestor R. Arista[2]

[1] Instituto de Astronomía y Física del Espacio-UBA-Conicet, Ciudad Universitaria, 1428 Buenos Aires, Argentina
[2] División Colisiones Atómicas, Centro Atómico Bariloche and Instituto Balseiro, 8400 S.C. Bariloche, Argentina

Abstract. A comparative study of the angular dispersion of slow muons in an electron gas is performed using three dielectric models which represent the case of metals (Lindhard model for a free electron gas) and the cases of semiconductors and insulators (Levine and Louie model and Brandt and Reinheimer model for systems with a band gap) and a non-linear model for both cases at very low velocities. The contribution of collective electronic excitations according to the dielectric model are found to be negligible. The results from the calculation using Lindhard expressions for the angular half width are coincident with the result of a multiple scattering model. In particular, the effects produced by the band gap of the material are analyzed in detail. Finally, as the recoil effect is negligible, there is an almost exact scaling, for a given velocity, between the proton and the muon results.

1 Introduction

Several studies of stopping powers, ranges and nuclear multiple scattering of MeV muons in solids have already been made, starting with the pioneering work of Lagerlund et al. [1] or the 4.1 MeV channeling experiments of Flik et al. [2]. However, low energy studies are more recent, such as the work of Valdés et al. [3] or the MUSCLE project [4,5]. With the advent of low energy muon beams capable of stopping in thin layers of crystalline material [6–9] it becomes important to know the depth distribution of these muons in order to properly interpret muon spin rotation experiments. These experiments are performed to learn more about the surrounding dipole contributions and the nature of local magnetic field distribution of a crystalline sample. Recent computational simulations [4,5] conclude that channeling conditions may increment the penetration depth, but these simulations do not take into account the importance of the multiple scattering of the projectile with the electrons of the channel. To our knowledge, no systematic analysis of angular distributions as a consequence of the multiple scattering of muons with electrons of the target, using different models appropriate for band-gap materials, have been made. The cases of interest include in particular different types of insulators or compounds with large band gaps, which are some of the basic materials of current interest for many of the experimental methods mentioned before.

In previous works [10,11] we developed a formalism based on the theory of multiple scattering and the calculus of the elastic scattering cross section for a dielectric model. A similar approach was formulated years later by another researchers [12]. Recently [13,14] we have also performed a comparative study of threshold effects in the energy loss moments of several projectiles using dielectric models for band gap materials. Combining both approaches, we aim now to describe the behaviour of the width of the angular dispersion of muons with a material characterized in terms of different dielectric approaches which represent the cases of metals (Lindhard free electron gas model [15,16]), semiconductors and insulators (Levine and Louie model [17] and Brandt and Reinheimer model [18,19] for systems with an energy band gap E_g). However, at low velocities non-linear effects become important. So we have incorporated the results using the non-linear approach [10], which applies also in the cases of very strong screening and large scattering amplitudes, and reduces to the linear treatment when the magnitude of the perturbation is small. The non-linear approach is based on transport cross section calculations according to quantum scattering theory. Finally, with the aid of these linear and non-linear models, we pay special attention to the appearance and the characteristics of threshold effects in the width of the multiple scattering angular distribution, since this band gap effect can play an important role at very low velocities to attenuate dechanneling.

The present work is organized as follows: in Section 2 we describe the dielectric approaches used in this study including the expressions for the multiple scattering function that can be applied to muons and protons. We also briefly describe the non-linear method. In Section 3 we analyze the results from all the methods, and compare with the results for protons. The conclusions are summarized in Section 4. The isotopic effects in Lindhard's expression are calculated for the first time in Appendix A. All the expressions have been written in atomic units.

[a] e-mail: archubi@iafe.uba.ar

2 Theoretical method

2.1 Multiple scattering formulation

The differential scattering probability for a projectile traversing an electron gas with velocity v and transferring a momentum q is given in the form [11]

$$\frac{d^4P}{d^3qd\omega} = \frac{e^2}{\pi^2q^2}\text{Im}\left[\frac{-1}{\varepsilon(q\cdot\omega)}\right]\delta\left(\hbar\omega - \hbar\overrightarrow{q}\cdot\overrightarrow{v} + \frac{\hbar^2q^2}{2M}\right) \tag{1}$$

where M is the mass of the incident particle and the last term in the delta function represents the recoil effect.

To solve equation (1) we first integrate over frequencies ω, and then separate the momentum transfer into parallel $q_{\parallel}$ and perpendicular $q_{\perp}$ components relative to the initial beam direction, $d^3q = d^2q_{\perp}dq_{\parallel}$. Integrating over $q_{\parallel}$ we get the differential probability of scattering for a muon of mass M traversing with velocity v an electron gas with an energy gap E_g and transferring a perpendicular momentum $q_{\perp}$ [11]:

$$\frac{dP}{dq_{\perp}}(q_{\perp},v,M) = \frac{2q_{\perp}Z^2}{\pi}\int_{q_{\min}}^{q_{\max}}\frac{dq_{\parallel}}{q^2}\text{Im}\left[\frac{-1}{\varepsilon(q,\omega)}\right]. \tag{2}$$

Two differences exist between this expression and that considered in reference [11] for the case of protons in a free electron gas. First, we must verify if it is possible to neglect the quadratic term in the maximum transferred energy $\varpi_{\max} = qv - \frac{\hbar q^2}{2m}$ (recoil effect) by a muon with incident energy $T = Mv^2/2$. The maximum transferred momentum to the electron taking into account the recoil effect is

$$q_{\max} = 2(v + v_F)\left(\frac{M+1}{M}\right). \tag{3}$$

This expression reduces to $q_{\max} = 2(v + v_F)$ when $M \gg 1$. Second, we must take into account the effect of the energy-gap. The lower limit of the integral is obtained from the frequency cut in the imaginary part of the dielectric function, i.e. $(q_{\parallel}v - \frac{q^2}{2M})^2 - E_g^2 > 0$. When $E_g = 0$ and $M \gg 1$ the lower limit of the integral reduces to 0 as in the case analyzed in reference [11].

2.2 Dielectric formalism

For all the linear cases considered in this work, the dielectric function of the material is expressed in terms of reduced variables in the following way (see Ref. [13] for further details):

$$\varepsilon(q,\omega) = 1 + g(z,E_g)[f_1(z,u,E_g) + if_2(z,u,E_g)] \tag{4}$$

where q and ω represent the momentum and energy transfers to the medium, and u and z are the corresponding reduced variables defined by the relations: $z = q/2q_F$, $u = \omega/qv_F$. E_g is the energy gap of the material ($E_g = 0$ for Lindhard dielectric function), and v_F and E_F are the Fermi velocity and corresponding energy. Other important

quantities to characterize the system are the electron density n, the plasma frequency $\omega_p = (4\pi n/m)^{1/2}$ and the electronic Wigner-Seitz radius $r_s = 1.919/v_F$. The probability of equation (1) can be separated into two contributions: $\frac{dP}{dq_{\perp}} = (\frac{dP}{dq_{\perp}})_{eh} + (\frac{dP}{dq_{\perp}})_{pl}$, corresponding to the excitation of single individual electrons, or electron-hole pairs $(\frac{dP}{dq_{\perp}})_{eh}$, and collective or plasmon excitations $(\frac{dP}{dq_{\perp}})_{pl}$, as explained in reference [13]. The calculation of the eh term is made by integrating equation (1) over the region of the $q-\omega$ plane where the imaginary part of $\varepsilon(q,\omega)$ is different from zero, while the calculation of the plasmon component requires a different procedure; in this case the integral can be transformed into a line integral along the resonance line corresponding to the plasmon dispersion curve defined by $\varepsilon(q,\omega) = 0$. This procedure is described in detail in references [11,14].

2.3 Non-linear model

To introduce the nonlinear approach in the present treatment we follow the procedure described in reference [10] with the following approximation for the imaginary part of the dielectric function at low velocities:

$$\varepsilon(q,\omega_0) = \begin{cases} \frac{2}{q^3}\omega, & q \leq 2k_F \\ 0, & q \geq 2k_F \end{cases} \tag{5}$$

with $\omega = \sqrt{(q_{\parallel}v - \frac{q^2}{2M})^2 - E_g^2}$ to include the band gap effect [17].

Replacing this expression in equation (2) we obtain:

$$\frac{dP}{dq_{\perp}} = \frac{2q_{\perp}Z^2}{\pi}\int\frac{dq_{\parallel}}{q}\left[\frac{\sqrt{(q_{\parallel}v - \frac{q^2}{2M})^2 - E_g^2}}{q^4|\varepsilon(q,E_g)|^2}\right]. \tag{6}$$

For the passage from dielectric formalism to non-linear formalism we use Nagy's replacement [20]:

$$\frac{1}{q^4|\varepsilon(q,E_g)|^2} = \frac{|f(\theta)|^2}{4} \tag{7}$$

where $f(\theta)$ is the non-linear quantum scattering amplitude, given by the partial wave expansion, as a function of the scattering angle θ. Using that $dq = (q_{\parallel}/q)dq_{\parallel}$ we insert equation (7) into equation (6) to obtain the differential scattering probability in the non-linear formalism:

$$\frac{dP}{dq_{\perp}}(q_{\perp},v,M) = \frac{2q_{\perp}Z^2}{\pi}\int_{q_{\min}}^{q_{\max}}dq$$
$$\times\left[\frac{\sqrt{((q^2-q_{\perp}^2)^{1/2}v - \frac{q^2}{2M})^2 - E_g^2}}{\sqrt{q^2-q_{\perp}^2}}|f(\theta)|^2\right] \tag{8}$$

where $q_{\min}$ is obtained from the condition of the frequency cut, i.e. the numerator of the integrand must be real, together with the condition that the minimum transferred energy in the laboratory system is given by $E_g = vv_r(1-\cos\theta)$ being v_r the relative muon-electron velocity [21].

2.4 Calculation of the angular distributions

Following the formulation of references [10,11] the electronic multiple-scattering function in the small-angle approximation for a projectile of mass M travelling a distance x with velocity v is:

$$fms(\alpha, x, v, M) = \int_0^\infty \kappa d\kappa J_0(\kappa\alpha) \exp\left[-x\mu_0(\kappa, v, M)\right]. \tag{9}$$

The function $\mu_0(\kappa, v, M)$ is determined from the previously defined scattering differential probability $\frac{dP}{dq_\perp}$ for the present case of an electron gas, by

$$\mu_0(\kappa, v, M) = \int_0^{q_{max}} \left[1 - J_0\left(\kappa\frac{q_\perp}{Mv}\right)\right] \frac{dP}{dq_\perp}(q_\perp, v, M)\frac{dq_\perp}{v} \tag{10}$$

where q_{max} is given by equation (3).

In the following we present a set of calculations of the angular width, considering a material described by $r_s = 1.5$, and energy gap values $E_g = 0$ and $E_g = 14$ eV. Similar properties may be expected for other values. Other cases of interest include semiconductors, such as Si and Ge, with r_s values close to 2 but much smaller energy gaps, so that threshold effects will be strongly reduced (see Ref. [13]). An alternative way to calculate the angular width of the MS distribution is by using a formula provided by [15]. However, the original Lindhard's formula does not include the recoil effect. Here we derived an extension of that formula which includes the recoil effect. This derivation is included in Appendix A of this paper.

3 Results

In Figure 1 we show some illustrative results for the angular width calculated using the three dielectric models considered here (Lindhard, Levine-Louie and Brandt-Reinheimer) in the case of muons traversing an electron gas characterized by $r_s = 1.5$. For low velocities we added the non-linear results. The difference between linear and non-linear results is significant. For dielectric models, we observe similarities between the behaviour of the angular width and the behaviour of the stopping calculated in reference [13]. In both magnitudes, in the presence of the band-gap, there is a velocity threshold $v \simeq 0.21$ a.u. In both magnitudes the B-R model gives lower results than the L-L model. For the angular width we observe that the energy band-gap effect becomes important for velocities less than 1 a.u. (2.8 eV). The calculations with the extension of Lindhard's formula derived in Appendix A are in full agreement with those obtained by the formulation of equations (8) and (9) in all the cases (i.e., for the three dielectric models), so they are represented by the same line in each case. The angular width scales as the square root of the distance x traversed by the projectile. Thus, to obtain the angular width in degrees from the figure it is necessary to multiply by the square root of the distance taking into account that the distance considered for our
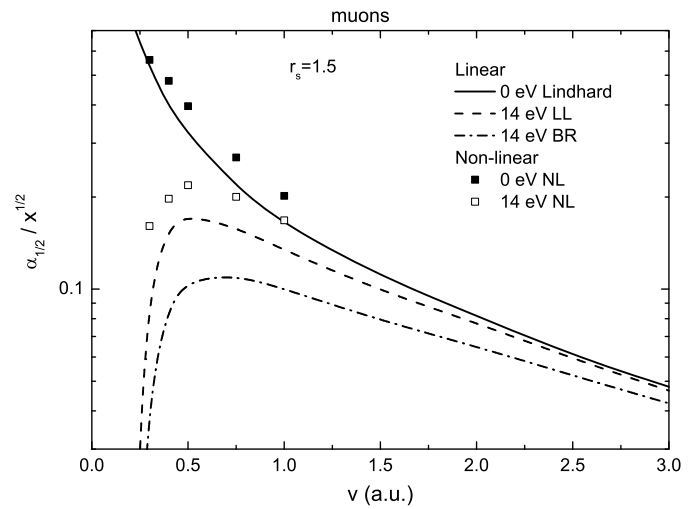

Fig. 1. Angular half width versus the projectile velocity for a muon impinging on a medium represented by an electron gas with $r_s = 1.5$ a.u. Comparisons between the three dielectric models: full-line, Lindhard model (energy gap = 0 eV), dashed-line, Levine-Louie model (energy gap = 14 eV), dashed-dotted line, Brandt-Reinheimer model (energy gap = 14 eV). Non-linear model: black squares, $E_g = 0$, empty squares, $E_g = 14$ eV. The angle is given in degrees while the depth is given in Angstroms.

calculus must be lower than the penetration depth for velocities around the threshold. Notice that the electronic stopping cannot be neglected when the traveled distance is near the penetration depth, but it can be assumed a constant velocity to obtain a lower quote for the estimation of the angular dispersion. For a more accurate estimation, the slowing down of the muons in the foil must be considered, taking into account the velocity dependence of the angular dispersion shown in Figure 1.

Finally, we have verified that the recoil effect and the plasmon contribution are negligible and that the linear results are consistent with those obtained with Lindhard's formula for the angular width [11] as in the case of protons. On the other hand, for low energies, it is expected that in insulators and semiconductors the muons captures an electron to form muonium. This neutral projectile would decreases the dispersion in a similar way that the angular width of the multiple scattering of hydrogen was lower than for protons [13]. As a consequence of this phenomena, we expect that in the experiments the effect of dechanneling would be attenuated for these materials.

3.1 Comparative results

In Figure 2 we show the non-linear results for the case examined in reference [5]. For 500 eV single charged ions, the critical angle for axial channeling in Fe can be estimated as $20°$ [22]. This estimation is affected by some uncertainty as it is shown in the work of Bergstrom et al. [23] for the case of a W target bombarded by protons. A precise value could only be obtained from experiments. The lower quote for the angular half-width is $\alpha_{1/2} = 2.8°$
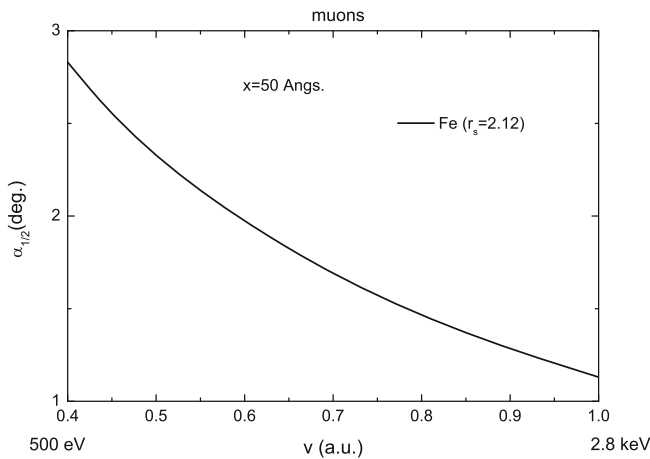
Fig. 2. Results for the angular half-width of muons traversing a Fe target of 50 Å represented by a free electron gas with $r_s = 2.12$ a.u.

for muons with an initial energy of 500 eV. Thus, this is a non-negligible value when the projectile is in a channeling situation, since the critical angle should be reduced to guarantee that the projectiles do not suffer dechanneling. However, for cases with a band-gap, as it happens with some semiconductors or insulators commonly used in the muon spin rotation experiments [5,7], at low velocities, the probability of dechanneling decreases as a consequence of the decreasing of the angular width near the gap. On the other hand, for low energies, it is expected that in insulators and semiconductors the muons captures an electron to form muonium. This neutral projectile would also decreases the dispersion in a similar way that the angular width of the multiple scattering of hydrogen was lower than for protons [13]. As a consequence of this phenomena, we expect that in the experiments the effect of dechanneling would be very attenuated for these materials.

In Figure 3 we compare the results of Figure 1 with the same results for protons for the linear models. In the case of protons, the angular half-width is very small and do not affect channeling conditions. Notice that the difference is one order of magnitude. As the recoil effect is negligible, there is an almost exact scaling, for a given velocity, between the proton and the muon results. This difference is intuitive if we assume that in Lindhard's formula the angular half-width behaves proportional to the inverse of the mass of the projectile when the recoil effect is negligible.

4 Conclusions

In channeling experiments, we knew that multiple scattering of protons with the electrons of the target lead to a negligible angular dispersion. However, in the case of muons, with a mass an order of magnitude lower than protons, electronic multiple scattering distributions significantly increase the dechanneling fraction of projectiles traversing a conductor modeled as a free electron gas. On the other hand, when the system is characterized by a band gap, the dechanneling decreases near the velocity
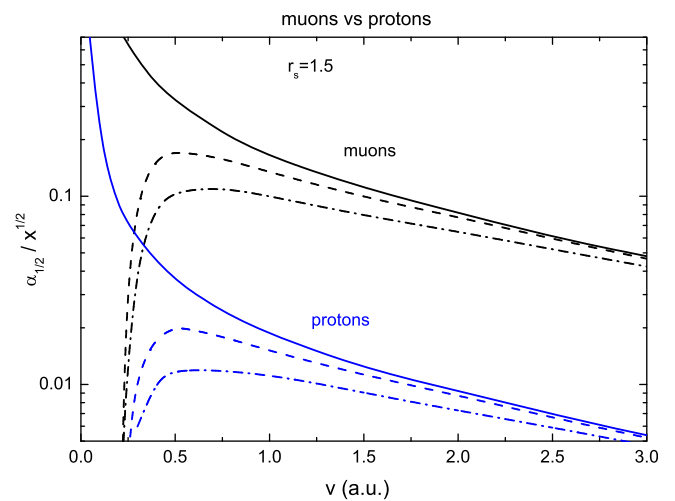

Fig. 3. Angular half width versus the projectile velocity for a projectile impinging on a medium represented by an electron gas with $r_s = 1.5$ a.u. Comparison between muons and protons. Full-line, Lindhard model (energy gap = 0 eV), dashed-line, Levine-Louie model (energy gap = 14 eV), dashed-dotted line, Brandt-Reinheimer model (energy gap = 14 eV).

threshold because of the reduction of the interaction between the projectiles and the electrons. Another important factor which contributes to this reduction is the formation of muonium at low velocities, whose angular dispersion must be reduced in a similar way to that of the angular dispersion of Hydrogen compared with protons, due to the structural similarities between the projectiles.

As a final consideration, we hope that this comparative study will be useful for applications in several cases of interest such as those mentioned at the beginning of this article.

Author contribution statement

Both authors contributed equally to the paper.

Appendix A: Extension of Lindhard's formula

In his original work of 1954 Lindhard included a formula for the angular spread produced by the multiple scattering of particles in a free electron gas [15], but the detailed derivation of this formula was not published. It may be shown that the Lindhard's expression applies to the case of heavy particles, such that $M \gg m$, so that recoil effects produced by the electron scattering are negligible small. Here we present a derivation of the angular spread which is an extension of Lindhard's formula for the general case of particles with arbitrary mass – i.e. where ratio m/M

is arbitrary – and which reduces to the Lindhard formula when $m/M \to 0$.

We start the derivation from the differential scattering probability given by equation (1)

$$\frac{d^4P}{d^3qd\omega} = \frac{e^2}{\pi^2 q^2}\text{Im}\left[\frac{-1}{\varepsilon(q\cdot\omega)}\right]\delta\left(\hbar\omega - \hbar\overrightarrow{q}\cdot\overrightarrow{v} + \frac{\hbar^2 q^2}{2M}\right) \tag{A.1}$$

where M is the mass of the incident particle and the last term in the delta function represents the recoil effect.

By definition this yields a scattering probability per unit time. Therefore, for an interaction time $\Delta t = \Delta x/v$ (being Δx a pathlength increase) the corresponding probability is

$$\begin{aligned}
\frac{d^4\widetilde{P}}{d^3qd\omega} &= \frac{d^4P}{d^3qd\omega}\Delta t \\
&= \frac{e^2\Delta x}{\pi^2 q^2 v}\text{Im}\left[\frac{-1}{\varepsilon(q,\omega)}\right]\delta\left(\hbar\omega - \hbar\overrightarrow{q}\cdot\overrightarrow{v} + \frac{\hbar^2 q^2}{2M}\right).
\end{aligned} \tag{A.2}$$

The transverse component of the momentum transfer in such scattering event is $\hbar q_\perp$, and so the scattering angle is $\alpha = \hbar q_\perp/Mv$.

We can then calculate the mean square value of the scattering angle after traversing a thickness Δx by

$$\langle\alpha^2\rangle = \frac{\hbar^2\langle q_\perp^2\rangle}{M^2 v^2} = \frac{\hbar^2}{M^2 v^2}\int q_\perp^2\frac{d^4\widetilde{P}}{d^3qd\omega}d^3qd\omega \tag{A.3}$$

This yields

$$\begin{aligned}
\langle\alpha^2\rangle = &\frac{\hbar e^2\Delta x}{\pi^2 M^2 v^3}\int\frac{q_\perp^2}{q^2}\text{Im}\left[\frac{-1}{\varepsilon(q,\omega)}\right] \\
&\times \delta(\omega - q_\parallel v + \gamma q^2)d^2q_\perp dq_\parallel d\omega
\end{aligned} \tag{A.4}$$

where $q_\parallel$ denotes the component of $\overrightarrow{q}$ parallel to $\overrightarrow{v}$ (being $q_\parallel^2 + q_\perp^2 = q^2$), and we introduce for convenience the parameter $\gamma = \hbar/2M$.

Performing the integration over ω and replacing $d^2q_\perp = 2\pi q_\perp dq_\perp$ we get

$$\langle\alpha^2\rangle = \frac{2\hbar e^2\Delta x}{\pi M^2 v^3}\int dq_\perp\int\frac{q_\perp^3}{q^2}\text{Im}\left[\frac{-1}{\varepsilon(q,\omega)}\right]dq_\parallel \tag{A.5}$$

with the relation $\omega = q_\parallel v - \gamma q^2 = q_\parallel v - \gamma(q_\parallel^2 + q_\perp^2)$.

Inserting here the relations

$$q_\parallel = q\cos\varphi$$
$$q_\perp = q\sin\varphi$$

(with $dq_\parallel dq_\perp = qdqd\varphi$), the integral becomes

$$\langle\alpha^2\rangle = \frac{2\hbar e^2\Delta x}{\pi M^2 v^3}\int q^2 dq\int\text{Im}\left[\frac{-1}{\varepsilon(q,\omega)}\right]\sin^3\varphi d\varphi \tag{A.6}$$

where now $\omega = q_\parallel v - \gamma q^2 = qv\cos\varphi - \gamma q^2$.

We can use now the variable $\eta = \cos\varphi$, so that $\sin^3\varphi d\varphi = (1-\eta^2)d\eta$, and then

$$\langle\alpha^2\rangle = \frac{2\hbar e^2\Delta x}{\pi M^2 v^3}\int q^2 dq\int\text{Im}\left[\frac{-1}{\varepsilon(q,\omega)}\right](1-\eta^2)d\eta \tag{A.7}$$

where now $\omega = qv\eta - \gamma q^2$.

In principle the variable $\eta = \cos\varphi$ could take values from –1 to +1. However since ω must be positive (energy transfer to the electron gas), the minimum value of η must be $\eta_{\min} = \gamma q/v$ (when $\omega = 0$), so η ranges from $\eta_{\min}$ to 1.

This formula seems quite appealing since η ranges in a very restricted domain. However the dielectric function is defined in the q, ω domain, and so it is convenient to make a final change of variables $\eta \to \omega = qv\eta - \gamma q^2$, replacing $d\eta = d\omega/qv$ and

$$\left(1-\eta^2\right) = 1 - (\omega + \gamma q^2)^2/q^2 v^2. \tag{A.8}$$

This finally yields:

$$\begin{aligned}
\langle\alpha^2\rangle = &\frac{2\hbar e^2\Delta x}{\pi M^2 v^4}\int_0^{q_{\max}}\frac{dq}{q}\int_0^{\omega_{\max}(q)}\text{Im}\left[\frac{-1}{\varepsilon(q,\omega)}\right] \\
&\times\left[q^2 - (\omega + \gamma q^2)^2/v^2\right]d\omega
\end{aligned}$$

and the corresponding mean value $\alpha_{1/2}$ is given by

$$\alpha_{1/2} = \sqrt{\langle\alpha^2\rangle\ln 2}.$$

In particular, for $\gamma = 0$ we retrieve the Lindhard's formula [15].

We notice that the maximum value of q in this integral is given by the condition $\omega_{\max}(q) = qv - \gamma q^2 \geqslant 0$, which yields $q_{\max} = v/\gamma$. For very massive particles, $\gamma \to 0$, and so $q_{\max} \to \infty$.

References

1. T.D. Lagerlund, M. Blecher, K. Gottow, R. Keller, W.C. Lam, Nucl. Instrum. Methods **120**, 521 (1974)
2. G. Flik et al., Phys. Rev. Lett. **57**, 563 (1986)
3. J.E. Valdés, P. Vargas, N.R. Arista, Nucl. Instrum. Methods Phys. Res. B **154**, 9 (2001)
4. N. Saquib, MUSCLE: A Simulation Toolkit Modeling Low Energy Muon Beam Transport in Crystals, Senior Projects Spring 2011, Paper 11, 2011
5. N. Saquib, W.J. Kossler, M. Deady, Phys. Proc. **30**, 42 (2012)
6. Y. Miyake et al., Phys. Proc. **30**, 46 (2012)
7. P. Bakule et al., Nucl. Instrum. Methods Phys. Res. B **266**, 335 (2008)
8. E. Morenzoni, *Physics and applications of low energy muons, Muon Science: Muons in Physics, Chemistry and Materials*, edited by S.L. Lee, S.H. Kilcoyne, R. Cywinski (Bristol and Philadelphia, 1999), Vol. 51, pp. 343–404
9. E. Morenzoni et al., Proceedings of the International Symposium on Science Explored by Ultra Slow Muon (USM), JPS Conf. Proc., Vol. 2, 2014, p. 0201
10. C.D. Archubi, N.R. Arista, Phys. Rev. A **72**, 062712 (2005)
11. C.D. Archubi, N.R. Arista, Phys. Rev. A **74**, 052717 (2006)

12. G. Maynard, C. Deutsch, EPJ Web Conf. **59**, 05020 (2013)
13. C.D. Archubi, N.R. Arista, Eur. Phys. J. B **89**, 86 (2016)
14. C.D. Archubi, N.R. Arista, Eur. Phys. J. B **90**, 18 (2017)
15. J. Lindhard, K. Dan. Vidensk. Selsk., Mat.-Fys. Medd. **28**, 1 (1954)
16. J. Lindhard, A. Winther, K. Dan. Vidensk. Selsk., Mat.-Fys. Medd. **34**, 1 (1964)
17. Z.H. Levine, S.G. Louie, Phys. Rev. B **25**, 6310 (1982)
18. W. Brandt, J. Reinheimer, Phys. Rev. B **2**, 3104 (1970)
19. W. Brandt, J. Reinheimer, Phys. Rev. B **4**, 1395 (1971)
20. I. Nagy, A. Arnau, P.M. Echenique, Phys. Rev. A **40**, 987 (1989)
21. L. de Ferrariis, N.R. Arista, Phys. Rev. A **29**, 2145 (1984)
22. Y.I. Ohtsuki, *Charged Beam Interactions with Solids* (Taylor and Francis, 1983)
23. I. Bergstrom, K. Bjorkqvisbt, B. Domeij, G. Fladda, S. Andersen, Can. J. Phys. **46**, 2679 (1968)